

Joint Rate and Power Control Algorithms for Wireless Networks

Ananth Subramanian and Ali H. Sayed, *Fellow, IEEE*

Abstract—There is a fundamental tradeoff between power consumption, data transmission rates, and congestion levels in a wireless network. These three elements influence the performance of rate and power control strategies, and they need to be coordinated judiciously. This paper proposes dynamic rate and power control algorithms for distributed wireless networks that also account for the congestion levels in a network. The design is pursued by formulating state-space models with and without uncertain dynamics and by determining control signals that help meet certain performance criteria (such as robustness and desired levels of signal-to-interference ratio). Simulation results illustrate the performance of the proposed control schemes.

Index Terms—Congestion control, Kalman filter, model uncertainties, power control, rate adaptation, robust filter, wireless networks.

I. INTRODUCTION

POWER consumption is a key limiting factor in the performance of wireless networks due to the presence of nodes with limited power capabilities. This limitation is further compounded by the fact that the nodes need to cater to certain data rates, which in turn require the SNR level and, consequently, the power level, to be above certain thresholds (in view of Shannon's capacity limit). In addition, the nodes need to be responsive to congestion conditions in the network, and therefore, they should be able to adjust their transmission rates and, hence, their power levels accordingly. It follows from these observations that a tradeoff exists between power levels, data rates, and congestion in a network. These three elements need to be coordinated in order to arrive at enhanced strategies that not only maintain a minimum variance between the actual and desired Signal-to-Interference (SIR) levels but that also ensure a low probability of packet loss in the network.

The interest in wireless networks in recent years has motivated the investigation of several power control strategies using different objective measures. For example, the strategies proposed in [1]–[4] balance the signal to interference ratios in a distributed way. The approaches from [5] and [6] include

quality of service (QoS) requirements, while the Kalman filtering approach from [7] uses admission control as the central quality-of-service (QoS) issue. A unified framework for the convergence analysis of some of these algorithms is proposed in [8]. These power control algorithms assume perfect measurements of SIR. Yet, perfect measurements are rarely available in practice, and hence, the work in [9] proposes a stochastic power control framework where noisy measurements are considered. With regards to the joint control of power and rate, one might consider at-least one of two strategies [10]–[14]. First, one could consider having a look up table containing rates and the corresponding power/SIR levels. For a given rate at which a node desires to transmit, the corresponding power and SIR levels could be read from the table. A second approach would be to transmit a pilot frame along with the data at any rate desired by the node. The node then increases the power level or reduces the rate if the pilot frame fed back to it by the receiving node is in error. While the first approach has the limitation of having to examine a lookup table, thus increasing time and complexity, the second approach suffers from time overhead. Rate-regulated methods like those given in [12] alleviate these problems. However, the methods assume perfect SIR measurements, and they do not cater to congestion mechanisms in situations like transport Control Protocol (TCP) over wireless settings. Actually, many of the available solutions do not combine in a cohesive manner the requirements of power, data rate, and congestion. For instance, the above solutions may not perform well when the desired data rates throughout the network need to vary due to the use of rate adaptation algorithms and congestion control algorithms. Allowing for such variable data rates and congestion control is desirable nowadays in view of the availability and affordability of wireless devices that support multiple data rates and the growing interest in TCP over wireless algorithms.

The purpose of this paper is to propose distributed strategies for the joint control of power and data rates in a wireless network by taking into account the congestion levels as well. We also allow the channel and interference gains to vary and assume incomplete knowledge of the underlying network dynamics. A useful feature of our presentation lies in showing how to model the network dynamics in terms of linear state-space models (by using, for example, a change of variables from the linear scale to the logarithmic scale). Once this is achieved, we then call upon quadratic control strategies to jointly control the power and data rate in the network. We also propose a robust algorithm to cater to the uncertainties in the state-space models.

Notation: For a column vector z , we write $\|z\|$ to denote its Euclidean norm. For a matrix C , we write $\|C\|$ to denote its maximum singular value.

Manuscript received July 10, 2003; revised January 17, 2005. This work was supported in part by the National Science Foundation under Grants ECS-0401188 and CCR-0208573. A short version of this paper appeared in [27]. The associate editor coordinating the review of this manuscript and approving it for publication was Prof. Gregori Vazquez.

A. Subramanian was with the Department of Electrical Engineering, University of California at Los Angeles, Los Angeles, CA 90095-1594 USA. He is now with the Institute for Infocomm Research, A-STAR, Singapore (e-mail: msananth@ieee.org).

A. H. Sayed is with the Department of Electrical Engineering, University of California at Los Angeles, Los Angeles, CA 90095-1594 USA (e-mail: sayed@ee.ucla.edu).

Digital Object Identifier 10.1109/TSP.2005.857044

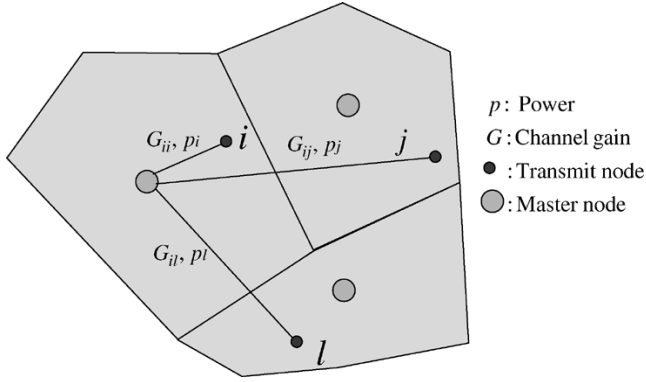


Fig. 1. Schematic representation with three cells, three master nodes, and active and interfering nodes. The active node is node i , and the interfering nodes are nodes j and l .

II. NETWORK MODEL

Consider a wireless network operating under dynamic network conditions. The space is divided into virtual geographical cells with each cell having one master node—see Fig. 1 for a schematic representation with three cells, three master nodes, and active and interfering nodes. A frequency slot is allocated to each node that wishes to communicate to the master node in a cell. The nodes communicating in the same frequency slot in other cells cause interference with this cell. The interference is measured in terms of the SIR, which is defined as follows. The SIR for node i at time k is defined by

$$\gamma_i(k) = \frac{G_{ii}(k)p_i(k)}{\sum_{j \in \mathcal{A}} G_{ij}(k)p_j(k) + \sigma_i^2} \quad (1)$$

where, for each time instant k , G_{ij} denotes the channel gain from the j th node to the intended master node of the i th node and is assumed to have a log-normal channel distribution, p_i is the transmission power from the i th node, and σ_i^2 is the power of the white noise at the receiver of the master node to which node i is connected. Moreover, \mathcal{A} denotes the set of all nodes that are interfering with node i from all cells.

III. ADAPTIVE POWER AND RATE CONTROL STRATEGY

Let $f_i(k)$ denote the flow rate (in bits per second per Hertz) at node i at time k . Here, k is the slot index and the channel gains are assumed to be constant during the slot. We shall initially assume that each node in the network employs a flow-rate control algorithm of the following form (see, e.g., [15]):

$$f_i(k+1) = f_i(k) + \mu [d(k) - c(k)f_i(k)] \quad (2)$$

where μ is a positive step-size, $c(k)$ is a measure of the amount of congestion in the network at time k , and $d(k)$ controls the amount of rate increase per iteration. In the absence of congestion (i.e., when $c(k) = 0$), the rate is increased by $\mu d(k)$. When congestion is present, the change in the rate is decreased by $\mu c(k)f_i(k)$ [15], [16]. Appendix A describes one method for estimating $c(k)$. In our subsequent derivations, we shall assume that $c(k)$ is independent of the flow rates at different nodes.

Equation (2) is a typical rate control strategy incorporated in computer networks. When there is no congestion or, equivalently, when the sender node receives the acknowledgment back from the final destination for every packet, then the sender increases the rate of transmission by increasing the frame size. This process is modeled by the additive term $\mu d(k)$. When there is congestion or, equivalently, when the sender node does not receive acknowledgment back from the final destination, it is assumed by the sender node that the packets that it sourced out have been lost in some link in the network. Hence, the source node reduces its rate by $\mu c(k)f_i(k)$. The value of $c(k)$ determines by how much the source node should reduce its rate. The $c(k)$ is normally user defined [17]—see Appendix A. The parameter $d(k)$ in (2) will be modeled as a random variable with mean m_d and variance σ_d^2 .

We shall assume that the receiving nodes have knowledge of the channel gains for decoding purposes. In practice, there will generally be a nonzero bit-error-rate (BER) at each receiver, and the value of the BER will depend on the SIR level. Now, given that we want to achieve a rate $f_i(k)$, at slot time k , a natural question is what SIR level we should aim for at the receiver in order to get close to this desired rate at a reasonable BER. Shannon's capacity formula suggests a plausible choice. The formula relates the maximum flow rate through a channel to the SIR level; even though it does not specify the code structure that would achieve the maximum rate.

Thus, ideally, and in view of Shannon's capacity formula, in order to achieve a flow rate of $f_i(k)$, it is necessary that the SIR level be at a value $\gamma'_i(k)$ related to $f_i(k)$ via

$$f_i(k) = \frac{1}{2} \log_2 [1 + \gamma'_i(k)]. \quad (3)$$

Note that we are using this expression to select $\gamma_i(k)$ from the given value of $f_i(k)$ (and not the other way around). Our objective is to design the power sequence $p_i(k)$ such that the actual resulting SIR level $\gamma_i(k)$, as measured by (1), would approach the desired SIR level $\gamma'_i(k)$, as defined by (3).

Let \bar{x} denote the decibel value of a variable x , namely, $\bar{x} = 10 \log x$. Now, usually, during normal network operation, $\gamma'_i(k) \gg 1$, and hence, $f_i(k)$ in (3) is proportional to $\bar{\gamma}'_i(k)$. Substituting this fact into (2), we find that if $f_i(k)$ is to vary according to (2), then the desired SIR level (in decibel scale) should vary according to the rule

$$\bar{\gamma}'_i(k+1) = [1 - \mu c(k)] \bar{\gamma}'_i(k) + \mu' d(k) \quad (4)$$

where $\mu' = 20\mu / \log_2(10)$.

Our aim is to select the power control sequence $\{p_i(k)\}$ such that the actual SIR levels $\{\gamma_i(k)\}$ will tend to (or track) the

¹When the actual SIR $\gamma_i(k)$ is less than the desired SIR $\gamma'_i(k)$, the receiver will not get the rate for which we are aiming, and the BER would grow for some coded systems. One way to alleviate this problem is to adjust (3) to include a buffer zone, namely, we could employ instead a relation of the form

$$\frac{f_i(k)}{\rho} = \frac{1}{2} \log_2 [1 + \gamma'_i(k)]$$

for some scaling factor $\rho < 1$. This additional factor ρ ends up being absorbed into the constant μ' after (4). The factor ρ would ensure that we have a higher value for the desired SIR level.

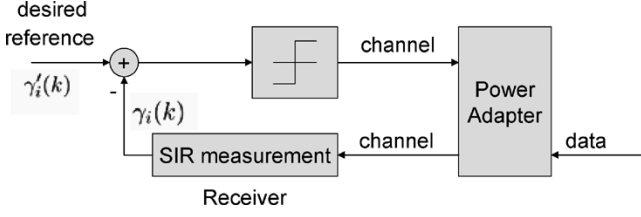


Fig. 2. Adaptive power control scheme.

desired levels $\{\gamma'_i(k)\}$. Our first scheme for attaining this objective borrows from known ideas on power control in wireless communications (see Fig. 2). In this scheme, the receiver measures the received power and compares it with a desired reference power. Based on this comparison, the receiver transmits a one-bit signal, known as the *power bit*, to the sender commanding it to increase or decrease its power. Here, we shall adopt the adaptive version developed in [18] due to its enhanced tracking ability. Thus, we assume that each node in the network adjusts its power according to the control algorithm:

$$p_i(k+1) = [\epsilon_i(k)]^{b_i(k)} p_i(k) \quad (5)$$

where $\epsilon_i(k) > 1$ is a parameter (usually between 1 and 2) that is allowed to vary from one node to another, and

$$b_i(k) = \text{sgn}[\gamma'_i(k) - \gamma_i(k)]. \quad (6)$$

This way, the power level in (5) is either scaled up or down according to whether $\gamma_i(k)$ is below or above the desired level $\gamma'_i(k)$. Furthermore, $\epsilon_i(k)$ is varied according to the rule

$$\begin{aligned} \text{If } |e(k+1)| < |e(k)|, \text{ then } \epsilon_i(k+1) &= \epsilon_i(k) - \varpi \\ \text{else } \epsilon_i(k+1) &= \epsilon_i(k) + \varpi \end{aligned}$$

for some small $\varpi > 0$, and where $e(k) = \gamma'_i(k) - \gamma_i(k)$.

The above adaptive method performs well when relatively accurate measurements of the SIR level $\{\gamma_i(k)\}$ are available and when small changes occur in the number of active nodes at any time. The performance, however, deteriorates when the number of active nodes vary considerably. For this reason, we now propose more elaborate joint rate and power control strategies.

Remark: Some power control algorithms, including the algorithms proposed in this paper, operate under the assumption that there exists a feasible set of power levels $\{p_i(k)\}$ such that the desired SIR can be met at all active nodes. By a feasible power level, we mean power values that lie within an interval $p_{\min} < p_i(k) < p_{\max}$. The nodes would drop out and stop their transmission if they are not able to meet the SIR requirement within the allowed power range. In the derivations that follow, we will not be imposing the power constraints for simplicity.

IV. QUADRATIC JOINT POWER AND RATE CONTROL STRATEGY

We continue to assume that each node in the network employs the flow-rate control algorithm (2) so that the desired SIR level

$\bar{\gamma}'_i(k)$ varies according to the rule (4). We shall further assume that each node in the network adjusts its power according to the power control algorithm

$$\bar{p}_i(k+1) = \bar{p}_i(k) + \alpha_i [\bar{\gamma}'_i(k) - \bar{\gamma}_i(k)] \quad (7)$$

where α_i is some given step-size parameter that is allowed to vary from one node to another.² Compared with the earlier scheme (5), we see by taking the logarithms of both sides of (5), and by using the fact that the logarithm is a monotonically increasing function, that (5) amounts to

$$\bar{p}_i(k+1) = \bar{p}_i(k) + \bar{\epsilon}_i(k) \text{sgn}[\bar{\gamma}'_i(k) - \bar{\gamma}_i(k)]. \quad (8)$$

In other words, the sign function is dropped from (7) in comparison to (8). Now, let

$$\beta_i(k) \triangleq \frac{G_{ii}(k)}{\sum_{j \in \mathcal{A}} G_{ij}(k) p_j(k) + \sigma_i^2}$$

denote the scaling factor that determines how $p_i(k)$ affects the achieved $\gamma_i(k)$ in (1), i.e.,

$$\gamma_i(k) = \beta_i(k) p_i(k)$$

or, equivalently, in decibel scale

$$\bar{\gamma}_i(k) = \bar{\beta}_i(k) + \bar{p}_i(k). \quad (9)$$

We shall refer to $\bar{\beta}_i(k)$ as the effective channel gain. We can derive a model for $\bar{\beta}_i(k)$ as follows. Let $J_i(k)$ denote the interference at node i , i.e.,

$$J_i(k) = \sum_{j \in \mathcal{A}} G_{ij}(k) p_j(k) + \sigma_i^2.$$

It has been indicated in the literature that $J_i(k)$ can be modeled as (e.g., [7], [19], [21], and [22]):

$$J_i(k+1) = J_i(k) z_i(k) \quad (10)$$

where $z_i(k)$ is a unit mean noise term. Here, $z_i(k)$ models the fluctuation in the interference levels when nodes either enter or leave the system or increase or decrease their power levels. Likewise, the dynamics of the channel gains $G_{ii}(k)$ can be modeled as (e.g., [7] and [19])

$$G_{ii}(k+1) = G_{ii}(k) m_i(k) \quad (11)$$

where $m_i(k)$ is again a unit mean random variable. The above models for the interference and the channel gains are similar to

²The ensuing analysis will be similar when $\log(1 + \gamma') \approx \gamma'$ (i.e., when γ' is sufficiently small). In this case, we will have no need for the updates to be in log domain. For example, we would update the power according to $p(k+1) = p(k) + \alpha(\gamma'(k) - \gamma(k))$.

those in [7] when the nodes are assumed stationary.³ Now, note that

$$\bar{\beta}_i(k) = 10 \log \left(\frac{G_{ii}(k)}{J_i(k)} \right).$$

Using (14), we get

$$\begin{aligned} \bar{\beta}_i(k+1) &= 10 \log \left(\frac{G_{ii}(k+1)}{J_i(k+1)} \right) \\ &= -10 \log J_i(k+1) + 10 \log G_{ii}(k+1) \\ &= -10 \log J_i(k) - 10 \log z_i(k) + 10 \log G_{ii}(k) \\ &\quad + 10 \log m_i(k) \\ &= 10 \log G_{ii}(k) - 10 \log J_i(k) + 10 \log m_i(k) \\ &\quad - 10 \log z_i(k) \end{aligned}$$

i.e., $\bar{\beta}_i(k)$ can be assumed to vary according to the random-walk model

$$\bar{\beta}_i(k+1) = \bar{\beta}_i(k) + n_i(k) \quad (14)$$

where $n_i(k) = 10 \log m_i(k) - 10 \log z_i(k)$ is a zero-mean disturbance of some variance σ_n^2 and is independent of $\bar{p}_i(k)$. Substituting this model for $\bar{\beta}_i(k)$ into (9), we find that the actual $\bar{\gamma}_i(k)$ varies according to the rule

$$\bar{\gamma}_i(k+1) = (1 - \alpha_i)\bar{\gamma}_i(k) + \alpha_i\bar{\gamma}'_i(k) + n_i(k). \quad (15)$$

Again, our objective is to design the power control sequence $\{p_i(k)\}$ such that the actual SIR levels $\{\gamma_i(k)\}$, as given by (15), will tend to the desired SIR levels $\{\gamma'_i(k)\}$, as defined by (4). We will derive the algorithm without the power constraints and assume that the nodes that are not able to achieve feasible power levels drop out of the system without transmission. We shall address this design problem by formulating a quadratic control problem as follows. First, we drop the node index i for simplicity of notation (it is to be understood that the resulting control mechanism is implemented at each node). Second, we introduce the two-dimensional state vector

$$x_k \triangleq \begin{bmatrix} \bar{\gamma}(k) \\ \bar{\gamma}'(k) \end{bmatrix}.$$

Then, combining (4) and (15), we arrive at the state-space model for x_k :

$$x_{k+1} = \begin{bmatrix} 1 - \alpha & \alpha \\ 0 & 1 - \mu c(k) \end{bmatrix} x_k + \begin{bmatrix} n(k) \\ \mu' d(k) \end{bmatrix}$$

or, more compactly

$$x_{k+1} = A_k x_k + w_k \quad (16)$$

³Indeed, a first-order Markov random model for the channel gains in the decibel scale is given by [7]

$$\bar{G}_{ii}(k) = \bar{G}_o + \delta \bar{G}_{ii}(k) \quad (12)$$

$$\delta \bar{G}_{ii}(k+1) = a \delta \bar{G}_{ii}(k) + \bar{m}_i(k) \quad (13)$$

where $\bar{m}_i(k)$ is white zero-mean Gaussian noise, and $a = 10^{-vT}/D$, with v being the velocity of the node, T the sampling time, and D the distance at which the gain falls to one tenth of its value near the source node. \bar{G}_o in the above equation is the bias value. From (12) and (13), we get

$$\bar{G}_{ii}(k+1) = a \bar{G}_{ii}(k) + (1-a)\bar{G}_o + \bar{m}_i(k).$$

When the nodes are stationary, i.e., when $a = 1$, we get (11). In a similar manner, by relying on the models proposed in [7], [19], we can justify (10).

where the 2×2 coefficient matrix A_k is given by

$$A_k = \begin{bmatrix} 1 - \alpha & \alpha \\ 0 & 1 - \mu c(k) \end{bmatrix} \quad (17)$$

and where w_k is a 2×1 random vector with covariance matrix

$$Q = E w_k w_k^T = \begin{bmatrix} \sigma_n^2 & \\ & \mu'^2 \sigma_d^2 \end{bmatrix}. \quad (18)$$

In order to drive $\gamma_i(k)$ toward the desired level $\gamma'_i(k)$, we shall introduce a control sequence $\{u_k\}$ into (16), as follows:

$$x_{k+1} = A_k x_k + B u_k + w_k \quad (19)$$

for some 2×2 matrix B and 2×1 control sequence u_k to be designed. For example, let

$$B u_k = \begin{bmatrix} u_p(k) \\ u_f(k) \end{bmatrix}$$

denote the individual entries of $B u_k$ to be designed. Then, the inclusion of the term $B u_k$ in (19) amounts to adding the control signal $u_p(k)$ to the power update (7). Likewise, the control signal $u_f(k)$ is added to the desired SIR update (4) [and, consequently, $(\log_2(10)/20)u_f(k)$ into the rate-flow update (2)].

In addition to employing a control sequence $\{u_k\}$, we shall assume for generality that we have access to output measurements that are related to the state vector as follows:

$$y_k = C x_k + v_k \quad (20)$$

for some known matrix C and where v_k denotes measurement noise with covariance matrix R

$$R = E v_k v_k^T.$$

Usually, $C = I$ so that the entries of y_k correspond to noisy measurements of the actual and desired SIR levels $\{\bar{\gamma}(k), \bar{\gamma}'(k)\}$.

We then seek a control sequence $\{u_k\}$ that minimizes the following stochastic quadratic cost function:

$$\mathcal{J} = \lim_{N \rightarrow \infty} \frac{1}{N} E \left\{ \sum_{k=0}^N [\lambda \|L x_k\|^2 + \|u_k\|^2] \right\}$$

where λ is a positive regularization parameter (chosen by the designer) and $L = [1 \ -1]$ (or some other more general choice). This particular choice of L results in

$$L x_k = \bar{\gamma}(k) - \bar{\gamma}'(k)$$

so that $\|L x_k\|^2$ is a measure of the energy of the difference between $\{\bar{\gamma}(k), \bar{\gamma}'(k)\}$. In this way, the cost function \mathcal{J} defined above is such that it seeks to minimize, on average, the squared Euclidean distance between the successive actual and desired SIR levels, as well as the energy of the control sequence itself. By varying the parameter λ , we can give more or less weight to the term $\|L x_k\|^2$ relative to $\|u_k\|^2$; larger values of λ give more relevance to $\|L x_k\|^2$.

The problem we are faced with is therefore to select the control sequence $\{u_k\}$ in order to minimize the cost function \mathcal{J} subject to the state-space constraint (19). Moreover, the solution $\{u_k\}$ should be a function of the available measurements $\{y_k\}$ only. The solution to this stochastic control problem is well-known [23], [24] and is known as the Linear Quadratic

Gaussian (LQG) solution. The solution is given by the following measurement feedback form. Start with $\hat{x}_k = 0$

$$P_0 = Ex_0x_0^T \triangleq \Pi_0, \quad P_\infty^c = 0$$

and iterate for all $k \geq 0$:

$$\begin{aligned} K_{c,k} &= (I + B^T P_k^c B)^{-1} B P_k^c A_k \\ K_{p,k} &= A_k P_k C^T (R + C P_k C)^{-1} \\ u_k &= -K_{c,k} \hat{x}_k \\ \hat{x}_{k+1} &= (A_k - K_{p,k} C) \hat{x}_k + K_{p,k} y_k + B u_k \\ P_{k+1} &= A_k P_k A_k^T + B Q B^T - K_{p,k} (R + C P_k C)^T K_{p,k} \\ P_k^c &= A_k^T P_{k+1}^c A_k + \lambda L^T L - K_{c,k}^T (I + B^T P_{k+1}^c B) K_{c,k}. \end{aligned}$$

Specifically, the solution employs two Riccati recursions: One is for P_k and runs forward in time, whereas the other is for P_k^c and runs backward in time. The variable P_k is used to compute the gain matrix $K_{p,k}$, which in turn is used to estimate the state vector from the observations y_k . On the other hand, the variable P_k^c is used to compute the gain matrix $K_{c,k}$, which is used to determine the optimal control sequence u_k . It should be noted that all matrix variables involved in the above recursions are 2×2 , and hence, the computational complexity involved in evaluating the solution is not significant.

The structure of the general solution can be simplified if we assume that the network is operating under conditions that are close to steady state. In this case, the congestion control function $c(k)$ would be assumed to have some steady-state value, say c , and consequently, the coefficient matrix A_k in (17) becomes a constant matrix A

$$A = \begin{bmatrix} 1 - \alpha & \alpha \\ 0 & 1 - \mu c \end{bmatrix}. \quad (21)$$

Under these circumstances, we can simplify the construction of the control sequence $\{u_k\}$ by replacing the Riccati recursions for $\{P_k, P_k^c\}$ by Riccati *equations*, i.e., by replacing $\{P_k, P_k^c\}$ by their positive-definite steady-state values $\{P, P^c\}$, which are obtained by solving the equations:⁴⁵

$$P = APA^T + BQB^T - K_p(R + CPC)^T K_p \quad (22)$$

$$P^c = A^T P^c A + \lambda L^T L - K_c^T (I + B^T P^c B) K_c \quad (23)$$

where now

$$K_c = (I + B^T P^c B)^{-1} B P^c A \quad (24)$$

$$K_p = APC^T (R + CPC)^{-1}. \quad (25)$$

Moreover

$$u_k = -K_c \hat{x}_k \quad (26)$$

$$\hat{x}_{k+1} = (A - K_p C) \hat{x}_k + K_p y_k + B u_k. \quad (27)$$

⁴Unique positive definite solutions $\{P, P^c\}$ are guaranteed to exist under mild stabilizability assumptions on the pairs $\{A, B\}$ and $\{A, L\}$ and detectability assumptions on the pairs $\{A, C\}$ and $\{A, B\}$. Moreover, the resulting closed-loop solution (26) and (27) will be stable—see [24].

⁵We assume the dynamics around an equilibrium point.

V. DEALING WITH DYNAMIC UNCERTAINTIES IN THE NETWORK

We now formulate a more general design procedure that takes into account uncertainties that arise due to the lack of perfect knowledge of the network conditions. For example, the congestion control function $c(k)$ is usually not known exactly and has to be estimated; the estimation process introduces errors into the assumed state-space model. In addition, modeling errors may arise from the fact that rate update (2) is ignoring delays due to round-trip times in the network. In order to pursue control design under such uncertainties in the models, we will replace the stochastic quadratic formulation of the previous section by a robust formulation that attempts to limit the influence of uncertainties on system performance.

Consider again the state-space model (19) and the corresponding coefficient matrix A_k in (17). We shall now assume that the congestion control function $c(k)$ is not known exactly due to modeling errors in the network. Specifically, we shall assume that

$$c_l \leq c(k) \leq c_u \quad (28)$$

for some known positive scalars $\{c_l, c_u\}$. In this way, the matrices $\{A_k\}$ themselves are not known exactly, but they can be modeled as $\bar{A}_k + \delta A_k$, where

$$A_k = \begin{bmatrix} 1 - \alpha & \\ 0 & 1 - \frac{\mu(c_l + c_u)}{2} \end{bmatrix} \quad (29)$$

and

$$\delta A_k = M \Delta_k D \quad (30)$$

with

$$M = 1, \quad D = \begin{bmatrix} 0 & 0 \\ 0 & \frac{\mu(c_u - c_l)}{2} \end{bmatrix}. \quad (31)$$

Moreover, Δ_k is in the interval $[-1, 1]$. We shall design the control sequence as follows. First, we use the robust algorithm of [25] to estimate the state of perturbed state-space models as in (26), (29), and (30). Let the state estimate be denoted by \hat{x}_k . Then, we design the control sequence $\{u_k\}$ as a function of these state estimates such that the effect of the noise disturbances $\{w_k, v_k\}$ on the error $\{\bar{\gamma}(k) - \bar{\gamma}'(k)\}$ is limited in the following manner:

$$E \left\{ \sum_{k=0}^{\infty} |\bar{\gamma}(k) - \bar{\gamma}'(k)|^2 \right\} < \nu^2 E \left\{ \sum_{k=0}^{\infty} (\|w_k\|^2 + \|v_k\|^2) \right\} + b \quad (32)$$

for some constant $b > 0$ and for the smallest possible ν^2 , and over all possible noise sequences $\{w_k, v_k\}$ and models $\{\bar{A}_k + \delta A_k\}$. In the above, E denotes the expectation operator. The solution is as follows—see Appendix B.

Robust Power and Rate Control Algorithm: Let

$$A_1 = \begin{bmatrix} 1 - \alpha & \alpha \\ 0 & 1 - \mu c_l \end{bmatrix}, \quad A_2 = \begin{bmatrix} 1 - \alpha & \alpha \\ 0 & 1 - \mu c_u \end{bmatrix}.$$

Given a 2×1 vector B and a 1×2 vector L , the following is a robust joint power and rate-flow control strategy:

- 1) Introduce a 2×2 matrix A_f and a 2×1 vector B_f (both to be determined).
- 2) Let $\hat{\lambda} = (1 + \bar{\kappa}) \|M^T C^T R^{-1} C M\|$, for some $\bar{\kappa} > 0$. In addition, let $\hat{R} = R - \hat{\lambda}^{-1} C M M^T C^T$, and define

$$\bar{C} \triangleq \begin{bmatrix} \hat{R}^{-\frac{1}{2}} C \\ \sqrt{\hat{\lambda}} D \end{bmatrix}$$

Determine the unique stabilizing and positive semi-definite solution P of the Riccati equation

$$P = A P A^T - A P \bar{C}^T (I + \bar{C} P \bar{C}^T)^{-1} \bar{C} P A^T + B Q B^T$$

and set

$$A_f = \hat{A} [I - P C^T R_e^{-1} C]$$

and

$$B_f = A_f P C^T \hat{R}^{-1}$$

where

$$\hat{A} = A \left[I - \hat{\lambda} \left(P - P \bar{C}^T \bar{R}_e^{-1} \bar{C} P \right) D^T D \right]$$

$$R_e = \hat{R} + C P C^T, \quad \bar{R}_e = I + \bar{C} P \bar{C}^T.$$

The matrix A_f is stable [25].

- 3) Using the just found $\{A_f, B_f\}$, define

$$\check{A}_1 = \begin{bmatrix} A_1 - B K_c & B K_c \\ A_1 - A_f - B_f C & A_f \end{bmatrix}$$

$$\check{A}_2 = \begin{bmatrix} A_2 - B K_c & B K_c \\ A_2 - A_f - B_f C & A_f \end{bmatrix}$$

$$\check{B} = \begin{bmatrix} I & 0 \\ I & -B_f \end{bmatrix}$$

for some 2×2 matrix K_c to be determined. Determine K_c , X , and the smallest ν^2 that guarantee

$$\begin{bmatrix} \check{H}_m & -\check{A}_m^T X \check{B} \\ -\check{B}^T X \check{A}_m & \nu^2 I - \check{B}^T X \check{B} \end{bmatrix} > 0$$

where

$$\check{H}_m = X - \check{A}_m^T X \check{A}_m - \check{L}^T \check{L}, \quad m = 1, 2$$

and

$$\check{L} = [L \quad 0]$$

(see Appendix B on how this inequality can be solved).

Then, set

$$u_k = -K_c \hat{x}_k$$

$$\hat{x}_{k+1} = A_f \hat{x}_k + B_f y_k + B u_k.$$

- 4) Partition $B u_k$ as

$$B u_k = \begin{bmatrix} u_p(k) \\ u_f(k) \end{bmatrix}$$

and update the rate flow and the power at the relevant node as follows, as long as $p_{\min} < p_i < p_{\max}$:

$$\kappa = \frac{(\log_2 10)}{20}$$

$$\bar{\gamma}'_i(k) = \frac{f_i(k)}{\kappa}$$

$$\bar{p}_i(k+1) = \bar{p}_i(k) + \alpha_i [\bar{\gamma}'_i(k) - \bar{\gamma}_i(k)] + u_p(k)$$

$$f_i(k+1) = f_i(k) + \mu [d(k) - c(k) f_i(k)] + \kappa u_f(k). \quad \diamond$$

VI. SIMULATION RESULTS

In order to illustrate the performance of the three proposed algorithms, we simulate a network using the model proposed in [19] for the channel gain from the i th node to its master node. In this model, G_{ii} has a lognormal distribution, namely

$$G_{ii} = S_0 d_{ii}^{-\psi} 10^{\frac{\phi}{10}} \quad (33)$$

where S_0 is a function of the carrier frequency, ψ is the path loss exponent (PLE), and d_{ii} is the distance of node i from its master node. The value of ψ depends on the physical environment and varies between 2 and 6 (usually 4). Moreover, ϕ is a zero mean Gaussian random variable with variance σ_ϕ^2 , which usually ranges between 6 and 12.

Let $g_i = \ln(G_{ii})$. Then, based on the above statistical characterization, the random variable g_i has a Gaussian distribution

$$f_{g_i}(g) = \frac{1}{\sigma_g \sqrt{2\pi}} e^{-\frac{(g-\bar{g})^2}{2\sigma_g^2}}$$

with mean

$$\bar{g} = \ln(S_0) - \psi \ln(d_{ii})$$

and standard deviation

$$\sigma_g = \frac{(\sigma_\phi \ln 10)}{10}$$

We shall neglect the effect of fast fading since the power update algorithm generally has a large time period. On the other hand, for the shadowing effect, we shall assume that the correlation sequence for the random process $\{g_i(k) = \ln G_{ii}(k)\}$ is given by

$$R_g(\tau) \triangleq E g_i(k) g_i(k - \tau) = \sigma_g^2 a^{|\tau|}, \quad a = 10^{-\frac{vT}{D}}$$

where σ_g^2 ranges between 3 and 10 dB, v is speed, T is the time period for channel probing, and D is the distance at which the normalized correlation reaches the value $1/10$. We assume that the velocity of the nodes is small enough so that we can approximate $a \approx 1$, and hence, $R_g(\tau) \approx \sigma_g^2$.

We then simulate a network consisting of nine cells with eight nodes per cell. Queries through nodes arrive at the master nodes with a poisson distribution with arrival rate θ . The service (or holding) time for each node is an exponential distribution with average holding time given by $1/\xi$. We consider a traffic load between 1 and 6 Erlang per cell, where the ratio of arrival rate

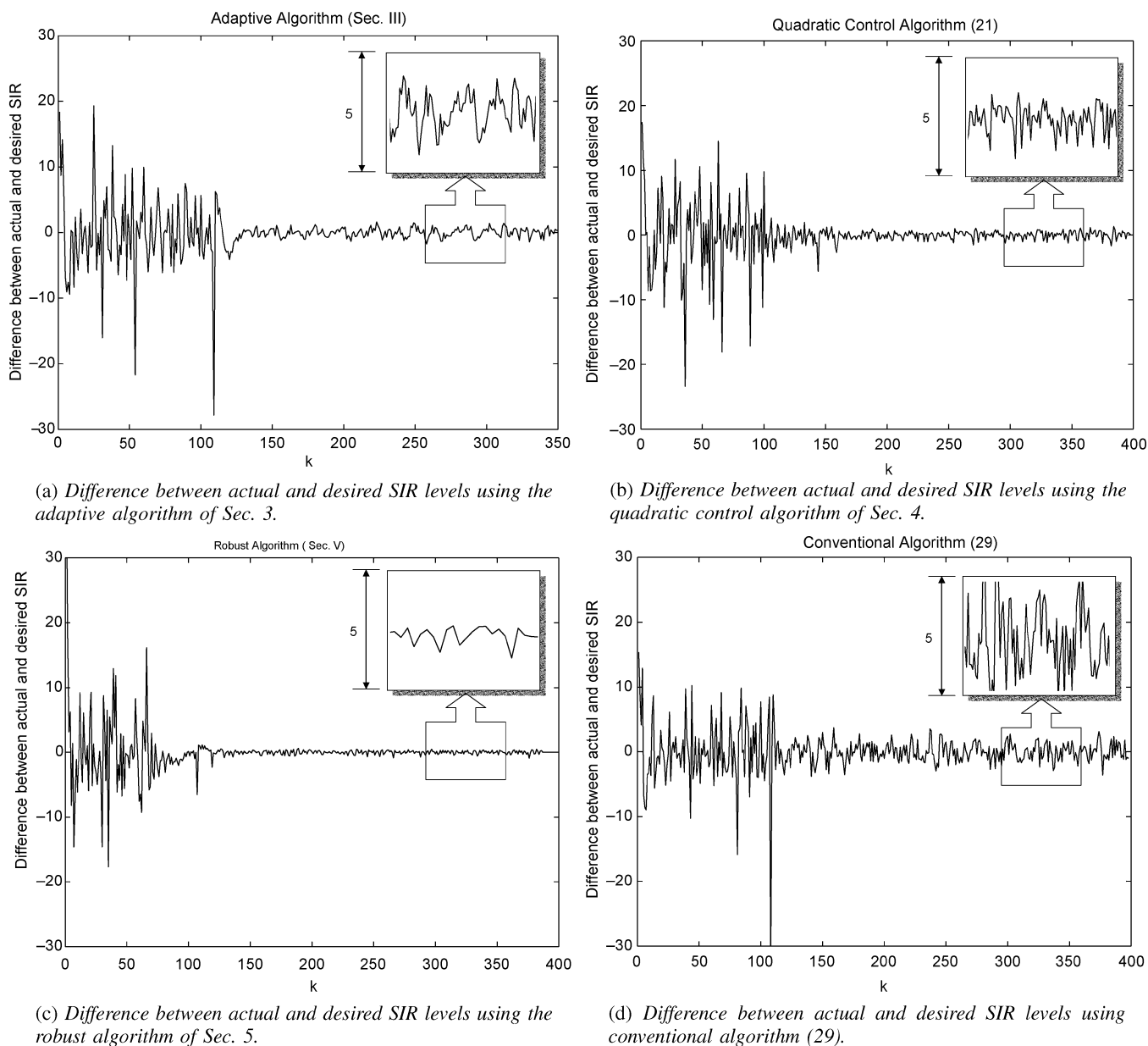


Fig. 3. Difference between actual and desired SIR levels using different algorithms.

to departure rate ($\theta/(\xi \times 9)$) denotes the traffic in Erlang per cell. New nodes need to have at least 12 dB SIR to get admission into the system. To maintain a uniform power distribution between nodes, we vary the master node randomly among the nodes. The maximum acceptable power that a node can transmit is the amount of power that causes the SIR level to reach 20 dB without any other user interference at a distance of 25 m. Once a node starts transmitting (or equivalently, a query has arrived at the master node according to Poisson distribution), it updates its power and rate jointly according to one of the algorithms given in Sections III–V, as long as it is connected with the master node. Once the master node has received the data from the node (or, equivalently, the node has been rendered service), the node departs.

To illustrate the performance of the adaptive algorithm of Section III, we assume that each node that wishes to transmit updates its rate of transmission as in (2). The value $c(k)$ is chosen

as a random variable for the purpose of simulations, assuming that the congestion levels in the network are random. It is chosen as a uniformly distributed random variable between 0 and 0.5. Moreover, $\mu d(k)$ is unit-mean with variance 0.001. Note that the tradeoff between rate, power, and congestion levels is addressed by considering them jointly in the rate and power control equations. The power and rate are updated in a combined manner, and the congestion levels enter the dynamics of the update equations in terms of $c(k)$. The nodes are made to adjust their power levels as according to (5). Each node transmits at a particular frequency slot. Under similar conditions as given above, we simulate the other rate and power control algorithms of Sections IV and V.

The plots in Fig. 3 illustrate the performance of the different algorithms. These plots show the difference between the actual SIR and the desired SIR. The smaller the difference in steady-state between the actual and desired SIRs, the better the

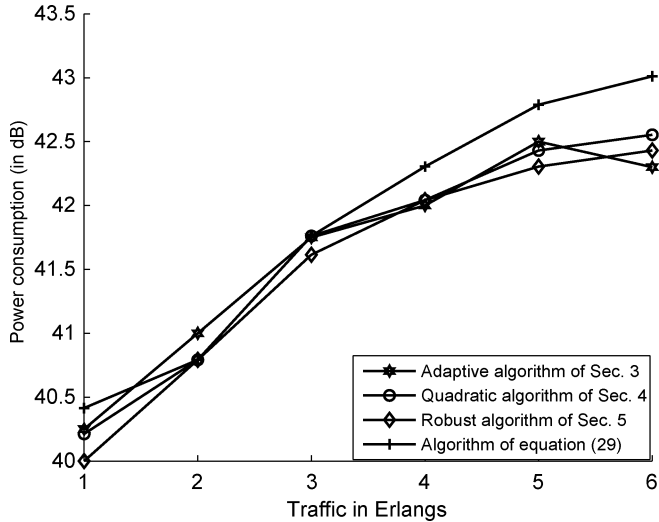


Fig. 4. Comparison of power levels for a desired SIR level of 6 dB. It is indicated that all algorithms consume essentially the same power.

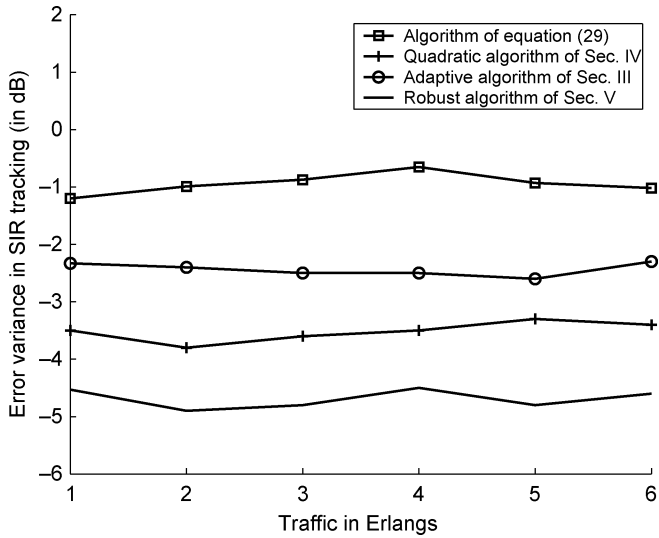


Fig. 5. Steady-state error variance in SIR tracking.

performance of the respective algorithms in tracking the desired SIR. In order to highlight the distinctions among the algorithms, each plot contains a smaller box that zooms in on steady-state values. Observe how the box in Fig. 3(c) contains values that range over a smaller interval when compared with the boxes in the other plots. All smaller boxes have the same maximum range of 5 for comparison purposes. In the figure, Fig. 3(a) illustrates the performance of the adaptive algorithm of Section III, and Fig. 3(b) illustrates the performance of the quadratic control algorithm of Section IV. The performance of the robust algorithm of Section V is shown in Fig. 3(c). Moreover, the following algorithm from [1]⁶

$$\bar{p}_i(k+1) = \bar{p}_i(k) + [\bar{\gamma}_i(k) - \bar{\gamma}'_i(k)] \quad (34)$$

which does not include a control term, performs as illustrated in Fig. 3(d). It is further noted in Fig. 4 that the power consumption is almost the same for (34) when compared with the other algorithms. It should be noted that the algorithms try to reduce the

⁶The algorithm (34) is the same as the algorithm in [1] when $\beta = 1$.

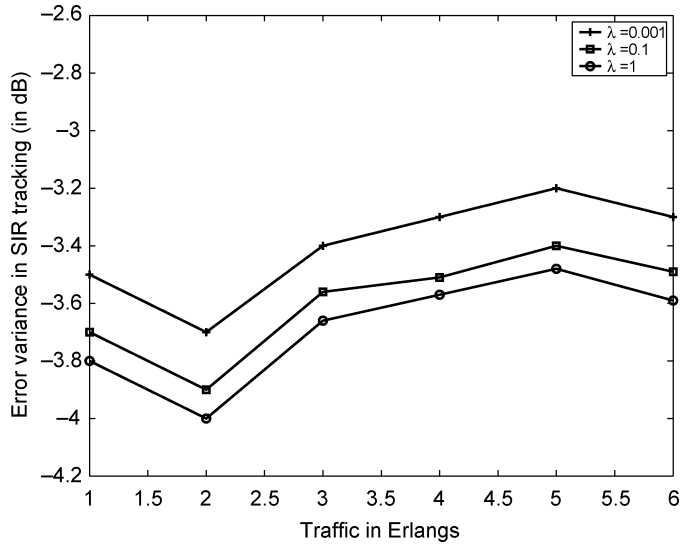


Fig. 6. Steady-state error variance in SIR tracking for the Quadratic algorithm using different values of λ .

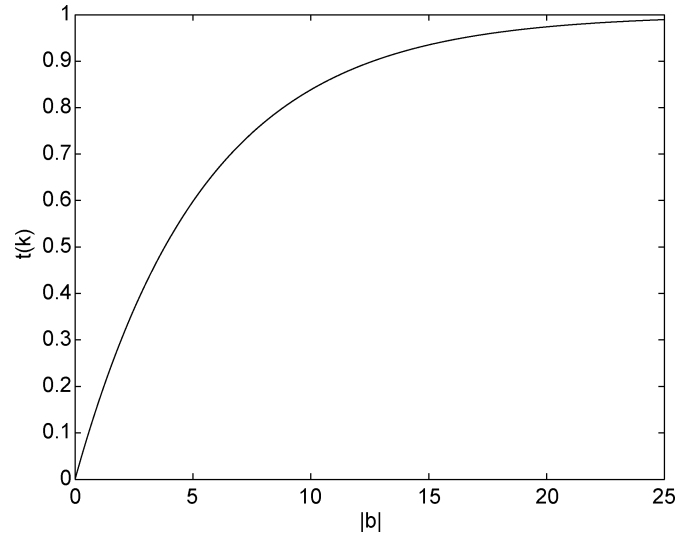


Fig. 7. Value of $t(k)$ as a function of $|b|$.

SIR error variance and not the power consumption. Hence, all the algorithms perform almost identically with respect to power consumption. The power consumption is given in terms of the ratio of power consumed to the floor noise power in decibels. For example, in the simulations, the average power consumed by a node at 1 Erlang traffic for the robust algorithm of Section V is 10, whereas the floor noise power is 10^{-3} . Hence, in decibel scale, the power consumed is shown in Fig. 4 as 40 dB.

Fig. 5 shows the performance of the algorithms in terms of the error variance in SIR tracking averaged over 350 experiments. It is seen that the proposed algorithms outperform (34). Fig. 6 shows the performance of the quadratic algorithm in terms of the error variance in SIR tracking averaged over 350 experiments for different values of λ .

VII. CONCLUSIONS

In this paper, we proposed three distributed rate and power control algorithms for wireless networks: 1) an adaptive scheme, 2) a quadratic control scheme, and 3) a robust scheme. All three

schemes consume essentially the same power as a function of network traffic (Fig. 4) and exhibit improved error variance between desired and actual SIR levels over the standard algorithm (34)—see Fig. 5. In addition, the robust solution of Section V exhibits the best performance among the four algorithms, albeit at an increased computational complexity. The adaptive solution of Section III is the least complex at some deterioration in performance. A key reason for the improved performance of the quadratic control and robust solutions over the adaptive solution is because the former algorithms are model-dependent. In other words, they exploit the underlying state-space models.

APPENDIX A CONGESTION ESTIMATION

We describe here a methodology by which $c(k)$ can be estimated at every iteration. Over a time period T , let

$$\Delta = f_i(k) - h_i(k) \quad (35)$$

where $h_i(k)$ is the end-to-end network bandwidth as estimated in [17]. In short, $h_i(k)$ is the rate at which bits are acknowledged by the destination node. We can then evaluate an end-to-end congestion measure $q(k)$ as follows:

$$\begin{aligned} \text{If } \Delta > \Delta_{\text{th}}, \quad \text{then } q(k) &= \frac{\Delta - \Delta_{\text{th}}}{\Delta} \\ \text{else } q(k) &= 0 \end{aligned}$$

for some positive threshold Δ_{th} . Let $b(k) = \gamma_{\text{ssd}} - \hat{\gamma}_i(k)$. Then, compute $c(k)$ as follows:

$$\text{If } \hat{\gamma}_i(k) > \gamma_{\text{ssd}}, \text{ then } t(k) = 0 \quad (36)$$

$$\text{else } t(k) = 1 - \psi^{b(k)} \quad (37)$$

$$c(k) = \epsilon q(k) + (1 - \epsilon)t(k) \quad (38)$$

for some $0 < \epsilon < 1$ and $\psi > 1$, and where γ_{ssd} is a desired steady-state SIR level, and $\hat{\gamma}_i(k)$ is a one-step-ahead predicted SIR at time k .

The value of $c(k)$ determines by how much the source node should reduce its rate. The $c(k)$ is normally user defined, as above [17]. The intuition behind such a $c(k)$ is as follows. The higher the rate at which the packets are sent by the source compared with the rate at which acknowledgment are received, the higher the value of $q(k)$ and, hence, the higher the value of $c(k)$. If $c(k)$ increases, then the rate $f_i(k+1)$ in (2) reduces, thus alleviating the level of congestion in the network. Another scenario in which the rate could reduce is when the estimate of the actual SIR present at the immediate receiving node is less than the desired SIR. Then, $t(k)$ increases, thus making $c(k)$ higher again. Fig. 7 shows a plot of $t(k)$ as a function of b . In other words, whenever there is congestion in the network or when the SIR level at the immediate receiving node is lower than it should be, the rate is reduced by the amount dictated by $\mu c(k) f(k)$.

For the algorithms of Sections IV and V, $\hat{\gamma}_i(k)$ is readily obtained from the Kalman and robust filters, respectively. For the algorithm of Section III, $\hat{\gamma}_i(k)$ can be obtained by estimating $\beta_i(k)$ as follows. Assume again that the effective channel gain varies according to model (14). Assume also that we have a noisy measurement $b(k)$ of $\beta_i(k)$, say $b(k) = \beta_i(k) + r(k)$,

with the variance of the measurement noise $r(k)$ equal to σ_r^2 . Then, the one-step predicted estimate of $\beta_i(k)$ can be obtained via the Kalman filter as follows. Start with $\hat{\beta}_i(0) = 0$, and iterate for all $k \geq 0$:

$$\begin{aligned} K_p(k) &= P(k) (\sigma_r^2 + P(k))^{-1} \\ \hat{\beta}_i(k+1) &= (1 - K_p(k)) \hat{\beta}_i(k) + K_p(k) b(k) \\ P(k+1) &= P(k) + \sigma_n^2 - \frac{P^2(k)}{(\sigma_r^2 + P(k))}. \end{aligned}$$

Then, $\hat{\gamma}_i(k) = \hat{\beta}_i(k) + \bar{p}_i(k)$.

APPENDIX B ROBUST PERFORMANCE

In this Appendix, we show that the algorithm of Section V is stable and ensures a robust performance level of ν^2 , as in (32). Define

$$\eta_k \triangleq \begin{pmatrix} x_k \\ \tilde{x}_k \end{pmatrix}, \quad o_k \triangleq \begin{pmatrix} w_k \\ v_k \end{pmatrix}. \quad (39)$$

Let $V(\eta_k) = \eta_k^T X \eta_k$, for some $X > 0$ to be determined in order to satisfy the inequality

$$EV(\eta_{k+1}) - EV(\eta_k) - \nu^2 E(w_k^T w_k + v_k^T v_k) + E\tilde{z}_k^T \tilde{z}_k < 0 \quad (40)$$

where $\tilde{z}_k = \tilde{L}\eta_k = \bar{\gamma}(k) - \bar{\gamma}'(k)$, with all the quantities as defined in Section V. We will show that for a given A_f and B_f , if X is determined such that the above inequality is satisfied, then (32) is guaranteed. Indeed, if we sum inequality (40) over k , and if we assume that the system is exponentially stable (which will be shown at the end of this appendix), we get for all $w_k, v_k \in l_2$

$$\begin{aligned} E \left\{ \sum_{k=0}^{\infty} \|\bar{\gamma}(k) - \bar{\gamma}'(k)\|^2 \right\} &< EV(\eta_0) \\ &+ \nu^2 E \left\{ \sum_{k=0}^{\infty} \|w_k\|^2 + \|v_k\|^2 \right\} \end{aligned} \quad (41)$$

as desired. Now, assume a control structure of the form

$$\hat{x}_{k+1} = A_f \hat{x}_k + B_f y_k + B u_k, \quad u_k = -K_c \hat{x}_k \quad (42)$$

for some given $\{A_f, B_f\}$ and unknown K_c . Combining this equation with

$$\begin{aligned} x_{k+1} &= (\bar{A}_k + \delta A_k) x_k + B u_k + w_k \\ y_k &= C x_k + v_k \end{aligned}$$

and assuming, for example, that $\bar{A}_k + \delta A_k$ is equal to one of the boundary points, say A_1 , we find that η_k satisfies the state-space model

$$\eta_{k+1} = \check{A}_1 \eta_k + \check{B} \begin{pmatrix} w_k \\ v_k \end{pmatrix} \quad (43)$$

where

$$\check{A}_1 = \begin{pmatrix} A_1 - BK_c & BK_c \\ A_1 - A_f - B_f C & A_f \end{pmatrix}, \quad \check{B} = \begin{pmatrix} I & 0 \\ I & -B_f \end{pmatrix} \quad (44)$$

and likewise for the boundary point A_2 . Using (43) and expanding (40) gives

$$\eta_k^T \check{A}^T X \check{A} \eta_k - \eta_k^T X \eta_k + \eta_k^T \check{A}^T X \bar{B} o_k + o_k^T \bar{B}^T X \check{A} \eta_k - \nu^2 o_k^T o_k + o_k^T \bar{B}^T X \bar{B} o_k + \eta_k^T \check{L}^T \check{L} \eta_k < 0. \quad (45)$$

With \check{A} taking values between \check{A}_1 and \check{A}_2 , condition (45) is equivalent to requiring

$$-\begin{pmatrix} \eta_k^T & o_k^T \end{pmatrix} \begin{bmatrix} \check{H}_m & -\check{A}_m^T X \bar{B} \\ -\bar{B}^T X \check{A}_m & \nu^2 I - \bar{B}^T X \bar{B} \end{bmatrix} \begin{pmatrix} \eta_k \\ o_k \end{pmatrix} < 0 \quad (46)$$

where

$$\check{H}_m = X - \check{A}_m^T X \check{A}_m - \check{L}^T \check{L}, \quad m = 1, 2.$$

Hence, (46) is satisfied if

$$\begin{pmatrix} \check{H}_m & -\check{A}_m^T X \bar{B} \\ -\bar{B}^T X \check{A}_m & \nu^2 I - \bar{B}^T X \bar{B} \end{pmatrix} > 0, \quad m = 1, 2 \quad (47)$$

for some K_c , ν^2 , and $X > 0$, as desired. Inequality (47) also implies that the system is stable because of the following. Note that for any boundary point \check{A}_m , the Lyapunov function $V(\cdot)$ satisfies, in the absence of noise

$$V(\eta_k) - V(\eta_{k+1}) = \eta_k^T (X - \check{A}_m^T X \check{A}_m) \eta_k \quad (48)$$

but inequality (47) implies that $\check{H}_m > 0$ for all \check{A} taking values between \check{A}_1 and \check{A}_2 . This in turn implies that $V(\eta_{k+1}) - V(\eta_k) < 0$ for all uncertainties. Hence, the process η_k is exponentially stable.

APPENDIX C OPTIMIZATION

We now show how to determine K_c , X and the smallest ν^2 in step 3 of the robust algorithm of Section V in order to guarantee (47). We shall restrict X to a block diagonal structure as

$$X = \begin{pmatrix} X_1 & 0 \\ 0 & X_2 \end{pmatrix}, \quad X_1 > 0, \quad X_2 > 0 \quad (49)$$

and define

$$Q = K_c X_2. \quad (50)$$

Now, through a Schur complementation argument, (41) is satisfied if

$$\begin{pmatrix} X & 0 & \check{A}_m^T X & \check{L}^T \\ 0 & \nu^2 I & \bar{B}^T X & 0 \\ X \check{A} & X \bar{B} & X & 0 \\ \check{L} & 0 & 0 & I \end{pmatrix} > 0. \quad (51)$$

Substituting (49) and (50) into the above inequality, we see that (41) holds for any given A_f and B_f , if there exist positive definite matrices $\{X_1, X_2\}$ and a matrix Q that satisfy

$$\begin{pmatrix} X_1 & 0 & 0 & 0 & A_m^T X_1 & C^T B_f^T X_2 & L^T \\ 0 & X_2 & 0 & 0 & Q^T & A_f^T X_2 & 0 \\ 0 & 0 & \nu^2 I & 0 & B^T X_1 & B^T P_2 & 0 \\ 0 & 0 & 0 & \nu^2 I & 0 & -B_f^T X_2 & 0 \\ X_1 A_m & Q & 0 & 0 & X_1 & 0 & 0 \\ X_2^T B_f C & X_2^T A_f & 0 & 0 & 0 & X_2 & 0 \\ L & 0 & 0 & 0 & 0 & 0 & I \end{pmatrix} > 0. \quad (52)$$

Finding the $\{X_1, X_2, Q\}$ that solve the above inequality for the smallest ν^2 is a convex optimization problem. Once $\{X_2, Q\}$ have been determined, K_c is obtained from $K_c = Q X_2^{-1}$.

APPENDIX D STABILITY OF THE NETWORK

Let J denote the set of sources (or equivalently nodes) in the network. Let r denote a route. Without loss of generality, we ignore routing choices and identify each source with a route. We consider first a single route and a single source scenario. Consider a particular source and a route r adopted by the source. The rate catered to by the route is proportionally given in terms of $\gamma'(k)$ (recall that the rate f_i is proportional to $\bar{\gamma}'(k)$). Now, the stability of η_k implies the stability of $\bar{\gamma}'(k) = [0 \ 1 \ 0 \ 0] \eta_k$. Hence, we will derive conditions for the stability of η_k , which will imply stability of $\gamma'(k)$ and, hence, that of route r . Consider again (43) in the absence of noises with \check{A} taking values in the polytope with vertices \check{A}_1 and \check{A}_2 :

$$\eta_{k+1} = \check{A} \eta_k \quad (53)$$

where

$$\check{A} = \begin{pmatrix} A_m - K_c & K_c \\ A_m - A_f - B_f C & A_f \end{pmatrix} \quad (54)$$

and A_m takes values in the polytope with vertices A_l and A_u . Now, the above matrix \check{A} is stable if

$$X - \check{A}_m^T X \check{A}_m > 0 \quad m = l, u \quad (55)$$

for some K_c and $X > 0$, but it can be seen that K_c and $X > 0$ satisfying (47) also satisfy (55). Condition (55) implies the asymptotic stability of the process $\{\eta_k\}$, and hence, the stability of route r is guaranteed.

For the scenario of multiple sources, when m sources use a route r , each of the sources being stable will contribute to a bounded arrival of packets in the route r , ensuring network stability.

ACKNOWLEDGMENT

The authors would like to thank N. Khajehnouri for his assistance with the simulations.

REFERENCES

- [1] G. J. Foschini and Z. Miljanic, "A simple distributed autonomous power control algorithm and its convergence," *IEEE Trans. Veh. Technol.*, vol. 42, no. 4, pp. 641–646, Nov. 1993.
- [2] —, "Distributed autonomous wireless channel assignment algorithm with power control," *IEEE Trans. Veh. Technol.*, vol. 44, no. 3, pp. 420–429, Aug. 1995.
- [3] J. Zander, "Distributed cochannel interference control in cellular radio systems," *IEEE Trans. Veh. Technol.*, vol. 41, no. 1, pp. 305–311, Mar. 1992.
- [4] S. A. Grandhi, R. Vijayan, and D. J. Goodman, "Distributed power control in cellular radio systems," *IEEE Trans. Commun.*, vol. 42, no. 2, pp. 226–228, Feb. 1994.
- [5] S. C. Chen, N. Bambos, and G. J. Pottie, "Admission control schemes for wireless communication networks with adjustable transmitted powers," in *Proc. IEEE INFOCOM*, vol. 1, Toronto, ON, Canada, 1994, pp. 21–28.
- [6] M. Andersin, Z. Rosberg, and J. Zander, "Gradual removals in cellular PCS with constrained power control and noise," *Wireless Networks*, vol. 2, no. 1, pp. 27–43, 1996.
- [7] K. Shoarinejad, J. L. Speyer, and G. J. Pottie, "A distributed scheme for integrated predictive dynamic channel and power allocation in cellular radio networks," in *Proc. GLOBECOM*, San Antonio, TX, 2001, pp. 3623–3627.
- [8] R. D. Yates, "A framework for uplink power control in cellular radio systems," *IEEE J. Sel. Areas Commun.*, vol. 13, no. 7, pp. 1341–1347, Sep. 1995.
- [9] S. Ulukus and R. D. Yates, "Stochastic power control for cellular radio systems," *IEEE Trans. Commun.*, vol. 46, no. 6, pp. 784–794, Jun. 1998.
- [10] M. K. Karakayali, R. Yates, and L. Razumov, "Joint power and rate control in multiaccess systems with multirate services," in *Proc. Conf. Inf. Sci. Syst.*, Baltimore, MD, Mar. 2003.
- [11] S. Kandukuri and S. Boyd, "Simultaneous rate and power control in multirate multimedia CDMA systems," in *Proc. Int. Symp. Spread Spectrum Technol. Applicat.*, Sep. 2000.
- [12] D. Kim, "Rate regulated power control for supporting flexible transmission in future CDMA mobile networks," *IEEE J. Sel. Areas Commun.*, vol. 17, no. 5, pp. 968–977, May 1999.
- [13] S. W. Kim and Y. H. Lee, "Combined rate and power adaptation in DS/CDMA communications over Nakagami fading channels," *IEEE Trans. Commun.*, vol. 48, no. 1, pp. 162–168, Jan. 2000.
- [14] S. A. Jafar and A. Goldsmith, "Optimal rate and power adaptation for multirate CDMA," in *Proc. IEEE Veh. Technol. Conf.*, vol. 3, Boston, MA, Sep. 2000, pp. 994–1000.
- [15] F. P. Kelly, "Models for a self managed internet," *Philos. Trans. R. Soc.*, vol. A358, pp. 2335–2348, 2000.
- [16] S. H. Low, "A duality model of TCP and queue management algorithms," *IEEE/ACM Trans. Networking*, vol. 11, no. 4, pp. 525–536, Aug. 2003.
- [17] R. Wang *et al.*, "Adaptive bandwidth share estimation in TCP Westwood," in *Proc. GLOBECOM*, Taipei, Nov. 2002.
- [18] M. Aldajani and A. H. Sayed, "Adaptive predictive power control for the reverse link channel," *IEEE Trans. Veh. Technol.*, vol. 52, no. 6, pp. 1447–1462, Nov. 2003.
- [19] M. Gudmundson, "Correlation model for shadow fading in mobile radio systems," *Electron. Lett.*, vol. 27, no. 23, pp. 2145–2146, Nov. 1991.
- [20] M. Aldajani and A. H. Sayed, "Stability and performance analysis of an adaptive sigma delta modulator," *IEEE Trans. Circuits Syst. II*, vol. 48, no. 3, pp. 233–244, Mar. 2001.
- [21] K. Leung, "Power control by interference predictions for wireless packet networks," *IEEE Trans. Wireless Commun.*, vol. 1, no. 2, pp. 256–265, Apr. 2002.
- [22] —, "A Kalman-filter method for power control in broadband wireless networks," in *Proc. IEEE INFOCOM*, vol. 2, New York, Mar. 1999, pp. 948–956.
- [23] K. J. Aström, *Introduction to Stochastic Control Theory*. New York: Academic, 1970.
- [24] T. Kailath, A. H. Sayed, and B. Hassibi, *Linear Estimation*. Englewood Cliffs, NJ: Prentice Hall, 2000.
- [25] A. H. Sayed, "A framework for state space estimation with uncertain models," *IEEE Trans. Autom. Control*, vol. 46, no. 7, pp. 998–1013, Jul. 2001.
- [26] A. Subramanian and A. H. Sayed, "Robust exponential filtering for uncertain systems with stochastic and polytopic uncertainties," in *Proc. CDC*, vol. 1, Las Vegas, NV, 2002, pp. 1023–1027.
- [27] —, "A stochastic control approach to power control in wireless networks," in *Proc. Workshop Statistical Signal Process.*, St. Louis, MO, Oct. 2003, pp. 391–394.



Ananth Subramanian (M'04) received the Bachelors degree in electrical and electronics engineering and masters degrees in mathematics in 1997 from BITS, Pilani, India. He received the Masters degree in electrical engineering and signal processing for communications from the Indian Institute of Science, Bangalore, in 1999 and the Ph.D. degree in electrical engineering in 2004 from the University of California, Los Angeles.

He is currently an Associate Scientist at the Institute for Infocomm Research, A-STAR, Singapore.

He has held the position of Teaching Fellow at UCLA. His areas of interests include statistical signal processing, wireless sensor, and *ad hoc* networks.

Dr. Subramanian was awarded the Gold Medal for being the best overall graduate student from the Indian Institute of Science and received the Henry Samueli Excellence in Teaching Award in 2002. He was also awarded the UCLA Chancellor's Fellowship in 2003.



Ali H. Sayed (F'01) received the Ph.D. degree in electrical engineering in 1992 from Stanford University, Stanford, CA.

He is Professor and Chairman of electrical engineering at the University of California, Los Angeles. He is also the Principal Investigator of the UCLA Adaptive Systems Laboratory (www.ee.ucla.edu/asl). He has over 200 journal and conference publications, is the author of the textbook *Fundamentals of Adaptive Filtering* (New York: Wiley, 2003), and is coauthor of the research

monograph *Indefinite Quadratic Estimation and Control* (Philadelphia, PA: SIAM, 1999) and of the graduate-level textbook *Linear Estimation* (Englewood Cliffs, NJ: Prentice-Hall, 2000). He is also co-editor of the volume *Fast Reliable Algorithms for Matrices with Structure* (Philadelphia, PA: SIAM, 1999). He has contributed several articles to engineering and mathematical encyclopedias and handbooks and has served on the program committees of several international meetings. He has also consulted with industry in the areas of adaptive filtering, adaptive equalization, and echo cancellation. His research interests span several areas, including adaptive and statistical signal processing, filtering and estimation theories, signal processing for communications, interplays between signal processing and control methodologies, system theory, and fast algorithms for large-scale problems.

Dr. Sayed received the 1996 IEEE Donald G. Fink Award, a 2002 Best Paper Award from the IEEE Signal Processing Society, the 2003 Kuwait Prize in Basic Science, the 2005 Frederick E. Terman Award, and co-author of two Best Student Paper awards at international meetings. He is also a member of the technical committees on Signal Processing Theory and Methods (SPTM) and on Signal Processing for Communications (SPCOM), both of the IEEE Signal Processing Society. He is a member of the editorial board of the IEEE SIGNAL PROCESSING MAGAZINE. He has also served twice as Associate Editor of the IEEE TRANSACTIONS ON SIGNAL PROCESSING, of which he is now serving as Editor-in-Chief. He is serving as General Chairman of ICASSP 2008.